Brain Research 1652 (2016) 135–143

Contents lists available at ScienceDirect

Brain Research

journal homepage: www.elsevier.com/locate/brainres

Research report

MiR-195 dependent roles of mitofusin2 in the mitochondrial dysfunction of hippocampal neurons in SAMP8 mice

Rui Zhang[a,b], Huimin Zhou[b,c], Lei Jiang[a], Yueran Mao[c], Ximing Cui[a], Bing Xie[a,b], Dongsheng Cui[a], Hui Wang[d], Qingfu Zhang[b], Shunjiang Xu[a,b,*]

[a] Central Laboratory, The First Hospital of Hebei Medical University, Shijiazhuang 050031, PR China
[b] Burn Engineering Center of Hebei Province, Shijiazhuang 050031, PR China
[c] Department of Endocrinology, The First Hospital of Hebei Medical University, Shijiazhuang 050031, PR China
[d] Department of Orthopedics, The First Hospital of Hebei Medical University, Shijiazhuang 050031, PR China

ARTICLE INFO

Keywords:
Alzheimer's disease (AD)
MicroRNA
SAM mice
Mitofusin 2 (mfn2)
Hippocampus
miR-195

ABSTRACT

Abnormal gene expression, including mRNAs, and microRNAs (miRNA), have been identified in the development of Alzheimer's disease (AD). Although mitofusin2 (mfn2) has been found to be down-regulated in the neurons from hippocampus and cortex in AD patients, little is known about its roles and the regulatory mechanisms in the pathogenesis of AD. This study was performed to investigate the roles of mfn2 protein and its upstream regulatory mechanism in the progression of AD using a senescence accelerated mouse prone-8 (SAMP8) model. The results of quantitative real-time PCR and western blot revealed that mfn2 expression displayed a consistent decrease with aging in the hippocampus of SAMP8 than did age-matched SAMR1 mice. The luciferase activity assay combined with mutational analysis confirmed the binding site of miR-195 to the 3′-untranslated region (3′-UTR) of mfn2 mRNA. Furthermore, miR-195 inhibitor or antigomir induced the higher level expression of mfn2 protein *in vitro* and *in vivo*. In addition, exogenous expression of miR-195 decreased the mitochondrial membrane potential (MMP) of the HT-22 cells by targeting mfn2. In conclusion, these results indicated that deregulation of mfn2 might be involved in mitochondrial dysfunction during the progression of AD, and its decreased expression was regulated at least in part by miR-195 in AD mice. The abnormal expression of miR-195 played a potential role in mitochondrial disorder by targeting mfn2 in hippocampus of SAMP8 mice. Therefore, upregulation of mfn2 protein by inhibiting miR-195 might be a potential new therapeutic strategy for treatment of AD.

1. Introduction

Alzheimer's disease (AD), a complex age-related neurodegenerative disease, is characterized by a variable degree of progressive loss of cognitive function. Although the precise mechanism of neurodegeneration in AD is not clear, there is a complex etiology is likely involved in multiple environmental, age-related, genetic, epigenetic, and inflammatory factors (Colangelo et al., 2002). Recent studies have shown that gene expression was deregulated in the hippocampus and cortex of AD patients and animal models during ageing, resulting in structural and functional damages (Liu et al., 2012; Manczak et al., 2011).

Mitofusin2 (mfn2), a mitochondrial fusion protein, is expressed mainly in tissues with high energetic requirements, such as brain, skeletal muscle, and heart (Chen et al., 2004). Several lines of evidence have demonstrated that mfn2 was not only involved in the modulating of mitochondrial shape and mitochondrial metabolism but also convinced to participate in the control of proliferation and apoptosis of various cells (Bucha et al., 2015; Chen et al., 2004; Guo et al., 2007; Wang et al., 2015). In addition, mfn2 is associated with the regulation of cell cycle progression, organelle shape and autophagy (Hailey et al., 2010). Multiple studies have established a link between the deregulated expression or mutation of mfn2 with some diseases, such as diabetes, cancer, and Charcot-Marie-Tooth diseases (Gao et al., 2012; Montecchiani et al., 2016; Wang et al., 2015). Our previous studies have demonstrated that the mRNA and protein levels of mfn2 were increased in the vascular smooth muscle cells (VSMC) during the cell redifferentiation (Zhang et al., 2010). More importantly, Manczak et al. reported that mfn2 mRNA and protein levels were down-regulated in the frontal cortex brain specimens from the patients at all Braak stages of AD progression (Manczak et al., 2011). Similarly, mfn2 protein levels were decreased in neurons from hippocampus of postmortem AD patients (Wang et al., 2009) and primary hippocampal cultures from

* Corresponding author at: Central Laboratory, The First Hospital of Hebei Medical University, No. 89, Donggang Road, Shijiazhuang 050031, PR China.
E-mail address: sjxu66@hotmail.com (S. Xu).

http://dx.doi.org/10.1016/j.brainres.2016.09.047
Received 4 July 2016; Received in revised form 27 September 2016; Accepted 29 September 2016
Available online 30 September 2016
0006-8993/ © 2016 Elsevier B.V. All rights reserved.

triple-transgenic (3×Tg) AD mice compared to nontransgenic (NTg) mouse neurons (Chen et al., 2016). The normal function of neurons requires mitochondrial synaptic terminals, which depending on the mitochondrial membrane dynamic properties. As one of the dynamin-related fusion proteins, mfn2 is involved in the maintenance of the dynamic balance of mitochondrial fusion and fission (Hollenbeck and Saxton, 2005). Moreover, it has been confirmed that mfn2 mutations disrupt axonal mitochondrial positioning and promote axon degeneration (Misko et al., 2012). The imbalance of mitochondrial fission/fusion has also been observed in the neurodegenerative diseases, such as AD (Corrado et al., 2012; Manczak et al., 2011). These reports suggested that mfn-2 is a key functional protein with regulatory and structural nature in brain, and plays an important role in the pathogenesis of AD. However, the upstream regulatory mechanisms of mfn2, especially at posttranscriptional level, still remain unclear.

MicroRNAs (miRNAs) have been implicated as important biological regulators of genes that regulate gene expression post-transcriptionally by translational repression or degradation of target mRNAs (Guo et al., 2010). It is estimated that more than one-third of all protein-coding genes are regulated by miRNAs in animals (Bartel, 2009). Although several researches have been focused on miRNA mediated regulation of mfn2 in human derived neuroblastoma cells and C2C12 myoblast (Bucha et al., 2015; Zhang et al., 2013), but there were no studies have been performed on the upstream regulation of mfn2 by miRNAs in the progression of AD.

Senescence accelerated mouse (SAM) is a murine model of accelerated aging, originally developed from breeding pairs of the AKR/J series. Of the senescence-accelerated mouse-resistant (SAMR) substrains, SAMR1 serves as a control exhibiting normal aging phenotype. Among the substrains of senescence-accelerated mouse-prone (SAMP), SAMP8 possesses the deficits in age-related learning and memory and shares phenotypes that resemble the symptoms of late-onset and age-related sporadic AD patients (Takeda et al., 1997). Therefore, SAMP8 mice are usually used as plausible aging-related neurodegeneration animal model to investigate the fundamental mechanisms of AD pathogenesis. Other and our studies have identified several AD-associated miRNAs using different strains of senescence accelerated mice (Liu et al., 2012; Zhang et al., 2014).

In the present study, we aimed to investigate whether mfn2 deregulation occurred in the development of AD, and whether such deregulation caused by post transcriptional regulation of miRNAs, using the senescence-accelerated mouse prone 8 (SAMP8). Our results suggested that mfn2 played an important role in the process of AD, and its downregulation was modulated by miR-195. This study might provide a potential new therapeutic strategy for treating AD by targeting mfn2.

2. Results

2.1. Expression of mfn2 in the cortex and hippocampus of SAMP8 mice

To determine the expression of mfn2 in the progression of AD, the mRNA and protein levels of mfn2 were firstly examined in the cortex and hippocampus of the SAMP8 mice aged 3-, 6-, and 9-month. As the characteristic feature of SAMR1 mouse was normal aging, so age-matched SAMR1 mice were used as control strain. The results from quantitative real-time PCR assay showed that the mfn2 mRNA levels

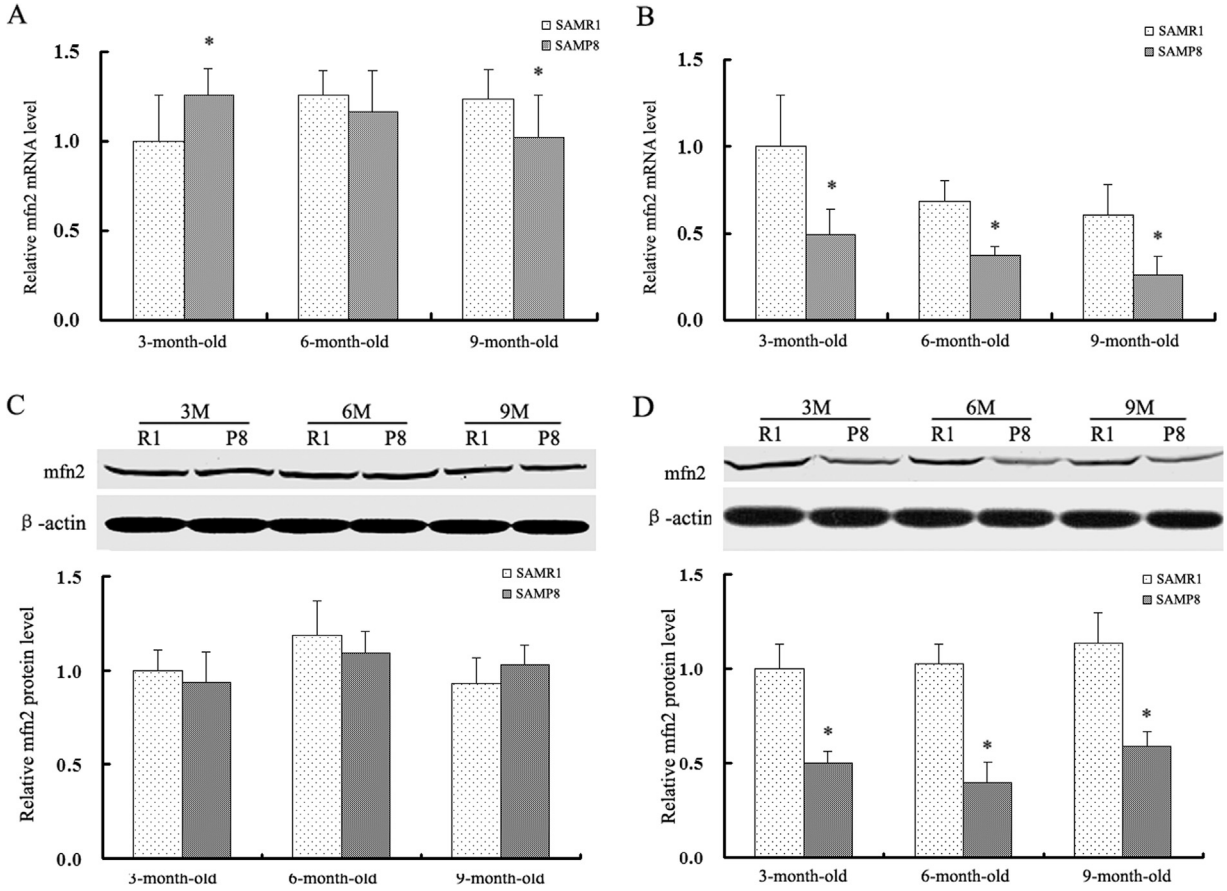

Fig. 1. Detection of mfn2 mRNA and protein levels in the cortex and hippocampus of SAMP8 and SAMR1 mice. Quantitative real-time RT-PCR analysis of the mfn2 mRNA levels in the cortex (A) and hippocampus (B) from 3-, 6-, and 9-month-old SAMP8 and SAMR1 mice. GAPDH was used as a control for the normalization of samples. Western blot analysis of mfn2 protein levels in cortex (C) and hippocampus (D) from 3-, 6-, and 9-month-old SAMP8 and SAMR1 mice. The β-Actin was used as a loading control. The values are the mean ± S.D. (n=6). *$P < 0.05$ *vs.* SAMR1 group.

were increased in the cortex of SAMP8 mice compared to SAMR1 mice at 3-months of age and decreased at 9-months of age ($P < 0.05$, Fig. 1A). However, western blot analysis showed that there were no significant changes in the levels of mfn2 protein in the cortex of 3-, 6-, and 9-month-old SAMP8 mice compared with age-matched SAMR1 mice ($P > 0.05$, Fig. 1C). In the hippocampus, both mfn2 mRNA and protein levels displayed a consistent decrease with aging in SAMP8 than did in age-matched SAMR1 mice ($P < 0.05$, Fig. 1B and D). To address the regional and cell-type specific distribution of mfn2 protein in the hippocampus, the tissue sections were subjected to immunohistochemical analysis. The results revealed a large number of cells that were immunoreactive for the mfn2 protein located in the CA3 subfield and a very small number of immunostained cells were observed in the CA1 and DG subfields in 6-month-old SAMP8 and SAMR1 mice (Fig. 2 upper). In addition, 6-month-old SAMP8 mice exhibited significant lower mfn2 levels than did the age-matched SAMR1 mice in the CA3 subfield of hippocampus (Fig. 2 lower)...

2.2. Initial screening of miRNAs targeting mfn2 in the hippocampus of SAMP8 mice

It was speculated in present study that the decrease of mfn2 protein levels in the hippocampus of SAMP8 mice with ageing might be due in part to the posttranscriptional regulation by miRNAs. In the initial screening of miRNAs targeting mfn2, we combined our previous microarray data and the results of prediction algorithms from Targetscan (www.targetscan.org) and miRanda (www. microrna.org) to predict the potential regulators of mfn2. The results of microarray showed that miR-195 and miR-15b were up-regulated in the hippocampus of SAMP8 mice (data not shown), as well as both of them got a higher predictive scores in the prediction algorithms. However, the results from quantitative real-time PCR assay showed that the miR-195 levels were increased ($P < 0.05$, Fig. 3A) in the hippocampus of 3- and 6-month-old SAMP8 mice compared with that in age-matched SAMR1 mice, whereas the miR-15b levels were

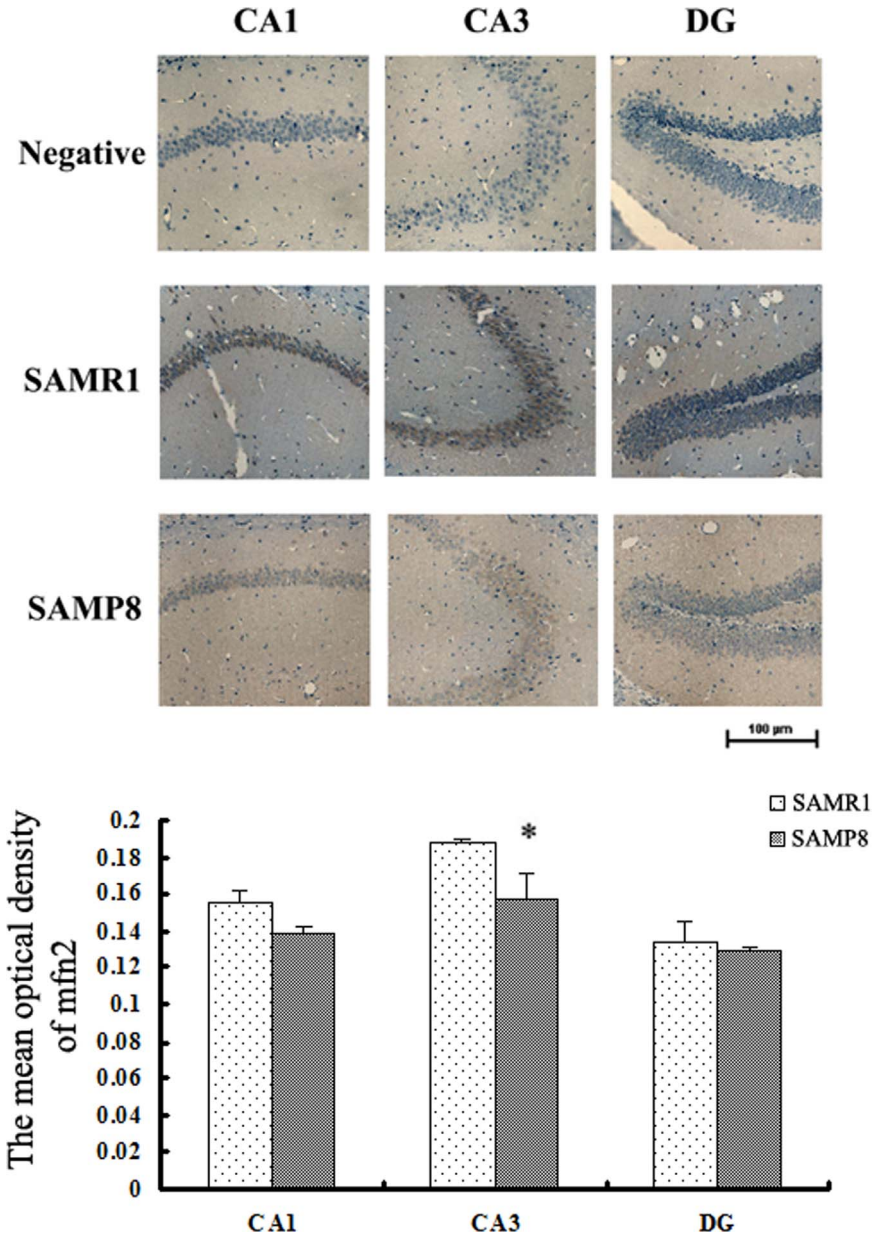

Fig. 2. Distribution of mfn2 protein in the hippocampus of senescence accelerated mice. Representative photos (upper) and quantitation of the signal levels (lower) of immunohistochemical staining of the mfn2 protein in the hippocampus from 6-month-old SAMR1 and SAMP8 mice. Negative: hippocampal sections from 6-month-old SAMR1 mice were immunohistochemical stained with preimmune rabbit IgG (1:500). The bar corresponds to 50 μm. *$P < 0.05$ *vs* SAMR1 group (n=6).

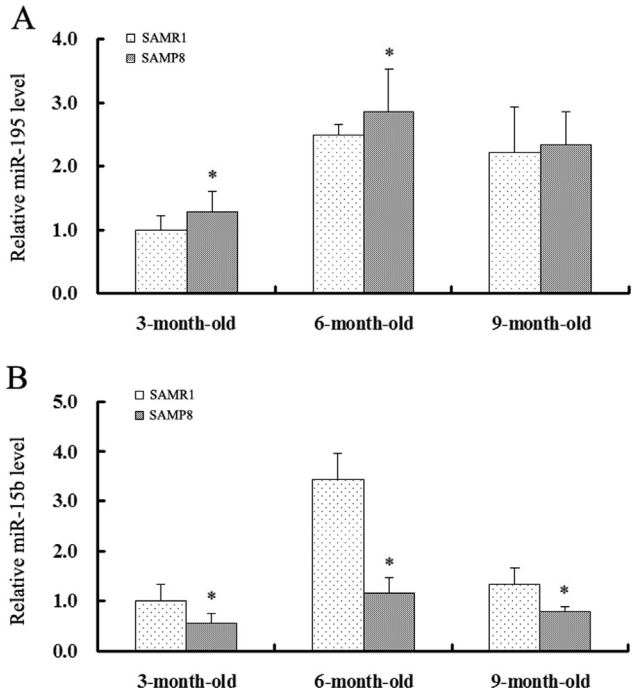

Fig. 3. Expression patterns of miR-195 and miR-15b in the hippocampus of SAMP8 and SAMR1 mice. Validation results of miR-195 (A) and miR-15b (B) in the hippocampus of 3-, 6-, and 9-month-old SAMP8 and SAMR1 mice by real-time RT-PCR analysis. *$P < 0.05$ *vs* SAMR1 group (n=6). U6-snRNA was used as a control for normalization of the samples.

decreased ($P < 0.05$, Fig. 3B) in hippocampus of 3-, 6-, and 9-month-old SAMP8 mice compared with that in age-matched SAMR1 mice..

2.3. *mfn2 was targeted by miR-195 through the predicted binding site*

The results of bioinformatic analysis revealed that the 3′-UTR of mfn2 mRNA harbors one potential targeting site of miR-195. To confirm the direct binding of miR-195 to 3′-UTR of the mfn2 mRNA, the luciferase reporter plasmids were generated containing the miR-195-binding site (WT vector) and its mutant sequence (MT vector). Then these reporter plasmids were cotransfected into 293A cells with miR-195 mimics, miR-195 inhibitor, or a scramble control, respectively. As expected, transfection with miR-195 mimics led to a significant reduction of luciferase reporter activity compared with scramble control ($P < 0.05$). When an inhibitor of miR-195 was used in place of miR-195 mimics, an increase was observed in luciferase activity ($P < 0.05$, Fig. 4A). However, the mutated sequences of mfn2 3′-UTR abrogated the repressive effect of miR-195 on the activity of its target 3′-UTR as measured by luciferase assay. Similarly, mutation of the predicted miR-195 binding site in the 3′-UTR of mfn2 abrogated the stimulative effects of miR-195 inhibitor on the luciferase reporter activity ($P > 0.05$, Fig. 4B). Scramble control elicited no effects on the luciferase reporter activity compared with the WT group or MT group ($P > 0.05$, Fig. 4A and B). These results indicated that miR-195 directly bound to 3′-UTR sequences of mfn2 mRNA..

2.4. *miR-195 regulated the expression of mfn2 at post-transcriptional level in HT-22 cells and hippocampal neurons*

To further validate whether miR-195 could regulate the expression of mfn2 at post-transcriptional level, we transfected miR-195 mimics, miR-195 inhibitor, or scramble control into HT-22 cells. The results showed that transfection of miR-195 mimics led to a significant increase of miR-195 levels compared with the scramble control ($P < 0.05$, Fig. 5A). In parallel, transfection of miR-195 inhibitor significantly decreased miR-195 levels compared with the scramble control ($P < 0.05$, Fig. 5B). However, mfn2 mRNA levels in HT-22 cells were not affected by the tansfection of miR-195 mimics or miR-195 inhibitor ($P > 0.05$, Fig. 5C and D). Meanwhile, mfn2 protein levels were decreased significantly by miR-195 mimics and increased by miR-195 inhibitor in HT-22 cells compared with scramble group ($P < 0.05$, Fig. 5E and F). To determine whether miR-195 could regulate the expression of mfn2 at post-transcriptional level in the animal model, mfn2 mRNA and protein levels were detected in the hippocampus of 6-month-old SAMP8 mice which were infused with the miR-195 antigomir or scramble into the lateral ventricle by quantitative real-time RT-PCR and western blot analysis, respectively. As expected, infusion of the miR-195 antigomir decreased the miR-195 levels ($P < 0.05$, Fig. 6A) and increased mfn2 protein levels ($P < 0.05$, Fig. 6C), but did not change the mfn2 mRNA levels in hippocampus of SAMP8 mice ($P > 0.05$, Fig. 6B), indicating that miR-195 inhibited the translation of mfn2 mRNA *in vivo*...

2.5. *Effects of miR-195 on the mitochondrial membrane potential (MMP) in the HT-22 cells*

Furthermore, the effects of miR-195 mimics on MMP in HT-22 cells were determined by using the JC-10 staining. The results showed that the ratio of JC-10 red to green fluorescence in HT-22 cells was significantly decreased after the transfection of miR-195 mimics ($P <$

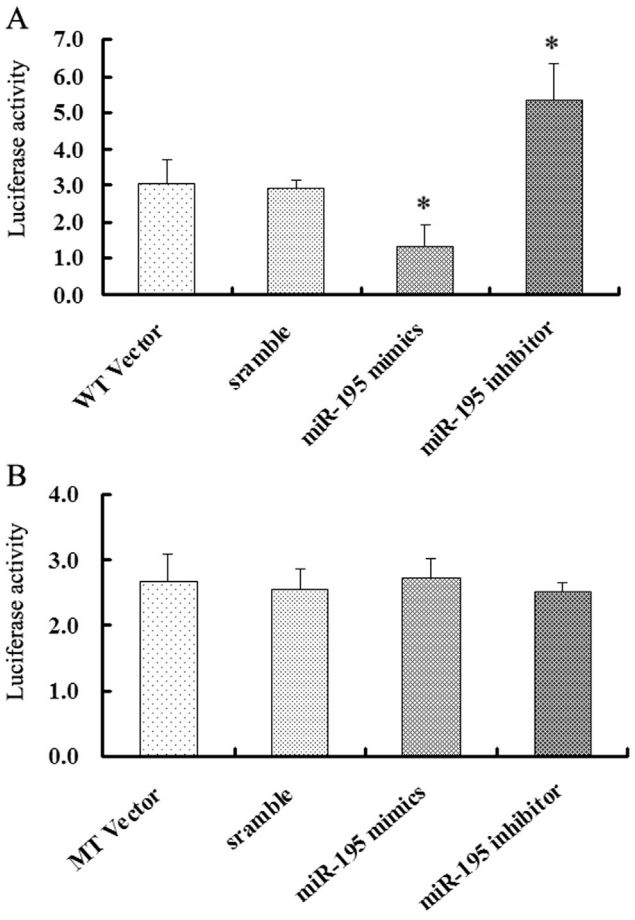

Fig. 4. MiR-195 directly targeted the 3′-untranslated region (UTR) of mfn2 mRNA. (A) Luciferase reporter assay in 293 A cells, showing the repressive effect of miR-195 mimics as well as the stimulative effect of miR-195 inhibitor on the activities of the mfn2 3′-UTR. *$P < 0.05$ *vs* WT or scramble group (n=3). (B) Mutation of the predicted miR-195 binding site in the mfn2 3′-UTR abrogated the repressive effect of miR-195mimics as well as the stimulative effect of miR-195 inhibitor on the activities of the mfn2 3′-UTR. *$P < 0.05$ *vs* MT or scramble group (n=3).

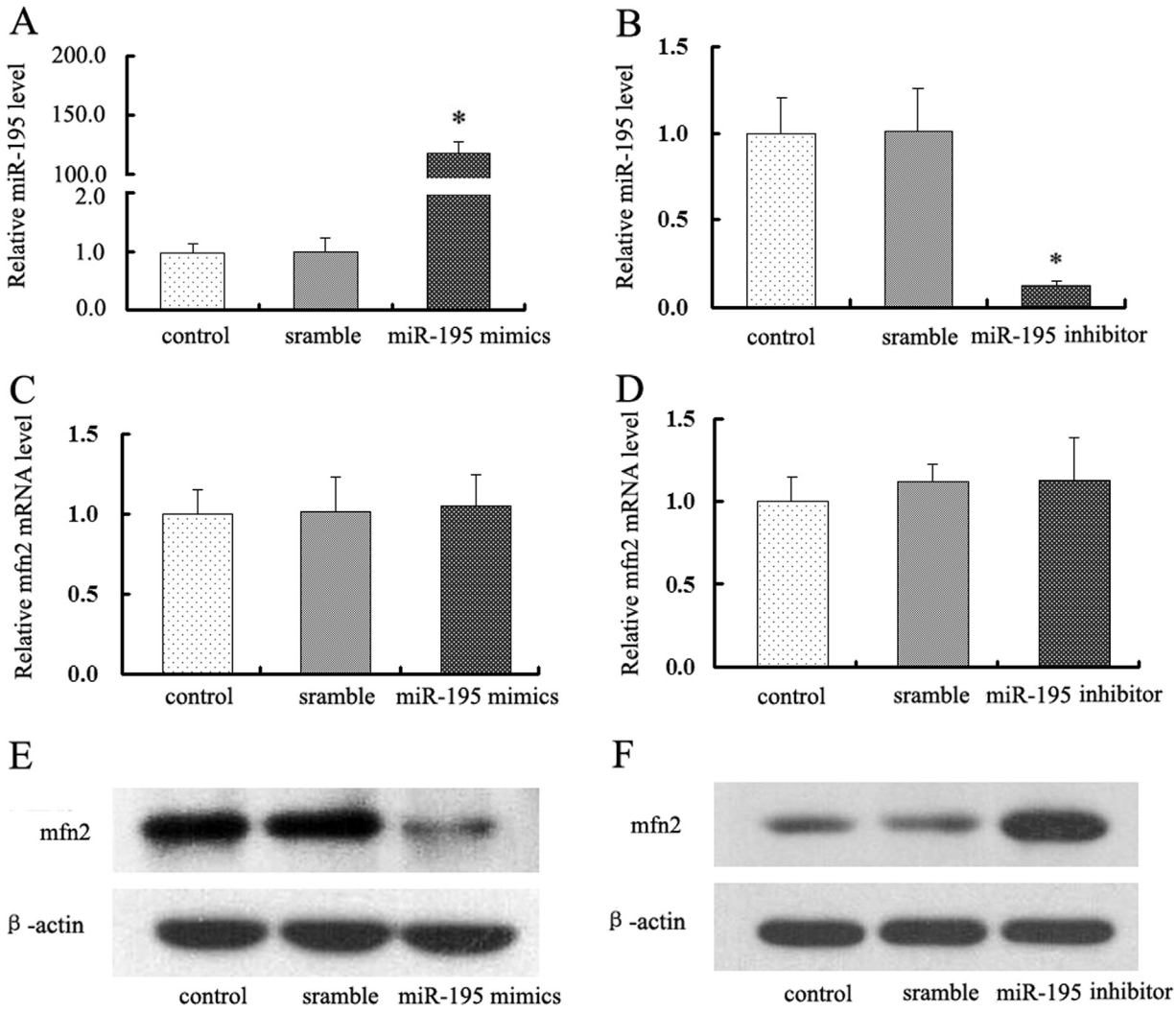

Fig. 5. MiR-195 negatively regulated the expression of mfn2 in HT-22 cells. HT-22 cells were transfected with miR-195 mimics or inhibitor for 24 h before harvesting. The levels of miR-195 (A and B) and mfn2 mRNA (C and D) in HT-22 cells following transfection. U6-snRNA or GAPDH was used as a control for the normalization of samples for quantitative real-time RT-PCR analysis. *$P < 0.05$ *vs* control or scramble. The mfn2 protein levels in HT-22 cells following transfection with miR-195 mimics (E) or miR-195 inhibitor (F). HT-22 cells were transfected with miR-195 mimics or inhibitor for 24 h; then, the cell lysates were subjected to western blotting antibodies against mfn2 and β-actin. β-Actin was used as a loading control. The values are the means ± S.D. (n=3). *$P < 0.05$ *vs* control or scramble group.

0.05, Fig. 7), indicating miR-195 resulted in the loss of MMP in HT-22 cells. No effects were found after transfection with scrambled miRNAs. The positive control carbonyl cyanide 3-chlorophenylhydrazone (CCCP) significantly decreased the ratio of JC-10 red to green fluorescence. However, transfection of miR-195 mimic together with AD-mfn2 infection prevented the loss of MMP induced by miR-195 mimics ($P < 0.05$, Fig. 7)..

3. Discussion

Alzheimer's disease (AD) is a complex neurodegenerative disorder. While the cause of AD remains unclear, an increasing body of evidences have identified that gene expression is deregulated in the development of AD. So it is necessary to identify the altered expression of genes in the neurons of different brain regions in AD patient or animal model for searching the diagnostic or therapeutic targets of AD. In this study, we found that the levels of mfn2 mRNA were decreased in the cortex and hippocampus of SAMP8 mice, however its protein levels were only decreased in the hippocampus of SAMP8 mice. These results indicated that the downreguolation of mfn2 protein has a very close relationship with the hippocampus-dependent cognitive function in AD process. Based on the results of bioinformatic analysis and our previous array data (Zhang et al., 2014), we selected two predicted miRNAs, miR-195 and miR-15b, to validate their levels of expression in the hippocampus of SAMP8 and SAMR1 mice, because of their higher predictive scores obtained from bioinformatic analysis. At last, we focused on miR-195 for its contrary expression trend to mfn2 in hippocampus of SAMP8. It was further confirmed that mfn2 was a direct target gene of miR-195 and the loss of MMP induced by miR-195 was dependent on the decreased expression of mfn2 protein in HT-22 cells.

It is generally accepted that mitochondrial dysfunction is a prominent feature of neurodegenerative diseases, including AD. A growing body of literatures supported that frequent fission and fusion are important for the maintenance of normal mitochondrial function (Hollenbeck and Saxton, 2005). Therefore, impairment of the mitochondrial fission and fusion balance has been regarded as a new mechanism of neurodegeneration (Knott and Bossy-Wetzel, 2008; Wang et al., 2009). More importantly, mitochondrial fusion has been reported to protect against neurodegeneration in the cerebellum (Chen et al., 2007). Mfn2, a dynamin-related protein with GTPase activity, affects the mitochondrial structure and mediates the mitochondrial function by regulating mitochondrial fusion (Bach et al., 2003; Martorell-Riera et al., 2014). In addition, mfn2 participates in the process of oxidative stress injury, an important pathologic mechanism

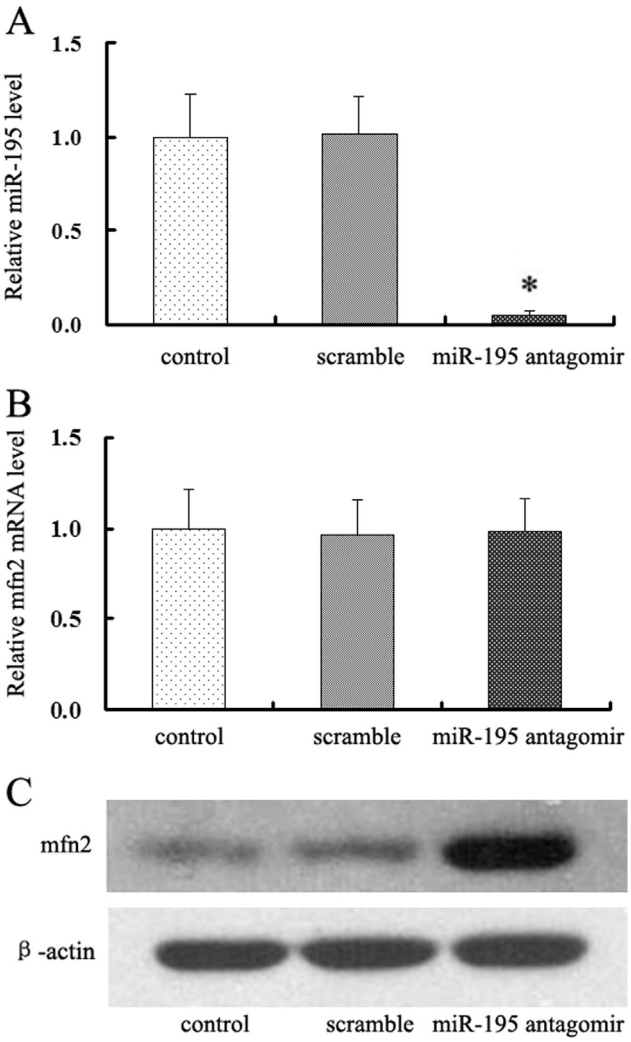

Fig. 6. Down-regulation of miR-195 increased mfn2 protein levels in the hippocampus of SAMP8 mice *in vivo*. The levels of miR-195 (A), mfn2 mRNA (B) and mfn2 protein (C) in the hippocampus of 6 month-old SAMP8 mice following infusion of miR-195 antigomir. The mice were sacrificed 48 h after the infusion of miR-195 antagomir, the levels of miR-195, mfn2 mRNA and mfn2 protein were detected by quantitative real-time RT-PCR and western blot analysis, respectively. U6-snRNA was used as a control for the normalization of samples for quantitative real-time RT-PCR analysis. The β-Actin was used as a loading control for western blot analysis. The values are the means ± S.D. (n=6). $^{*}P < 0.05$ *vs* control or scramble group.

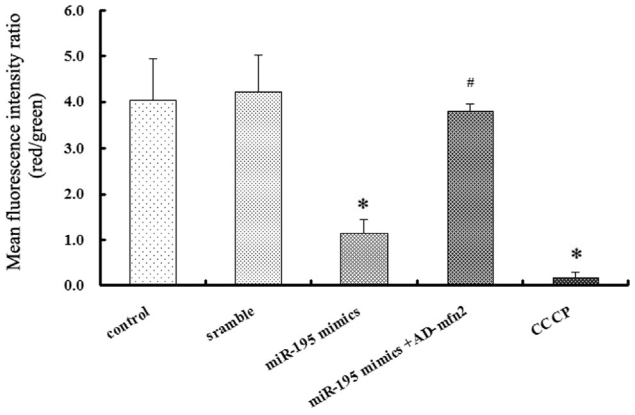

Fig. 7. Effect of miR-195 mimics on mitochondrial membrane potential (MMP) in the HT-22 cells. After transfection with scramble controls, miR-195 mimics, or the combination of miR-195 mimics and AD-mfn2 or treatment with Carbonyl cyanide 3-chlorophenylhydrazone (CCCP) for 24 h, the MMP in HT-22 cells was assessed by using JC-10. The ratio of red/green fluorescence intensity was used to determine the values of MMP. CCCP was used as a positive control for the loss of MMP. Data were expressed as mean ± SEM. $^{*}P < 0.05$ *vs* control or scramble group; $^{\#}P < 0.05$ *vs* miR-195 mimic group (n=3).

for AD. It was reported that mfn2 expression was decreased when Neuro-2a (N2a) cells exposed to Aβ oligomers (AβOs)-mediated oxidative stress, and over-expression of mfn2, but not mfn1, significantly inhibited the AβO-mediated neuronal cells death pathway (Park et al., 2015). Similarly, treatment cells with antioxidant probucol significantly increased mfn2 protein levels in AD cybrids compared to the vehicle-treated cells (Gan et al., 2014). Besides, a number of reports suggested that mfn2 played important roles in autophagy and apoptosis (Guo et al., 2007; Zhao et al., 2012), which closely related to the development of AD. These observations have allowed us to propose that mfn-2 plays a relevant role in the etiology of AD. In this study, it was confirmed that mfn2 was down-regulated in the hippocampus of SAMP8 mice, and mfn2 protein mainly located in the CA3 subfield of the hippocampus, an area that is closely related to modulation of learning and memory. Since the importance of hippocampus has been universally recognized in the modulation of cognitive function, the decreased expression of mfn2 protein in the hippocampus might play a key role in the development of AD. Thus, it is necessary to reveal the molecular mechanisms by which mfn-2 expression is regulated during the progression of AD.

Our previous study has reported that mfn2 expression was activated by the interaction of Krüppel-like factor 4 with p300 in VSMC (Zhang et al., 2010). Other people's studies have shown PGC-1α coactivated by ERR-α, participated in the stimulation of mfn2 expression in skeletal muscle cells (Soriano et al., 2006). MicroRNAs (miRNAs) are a class of small non-coding RNA molecules that regulate gene expression post-transcriptionally by translational repression or degradation of target mRNAs. MiR-106b and miR-214 have been found to target the 3′ -UTR of mfn2 (Bucha et al., 2015; Zhang et al., 2013). Some evidence indicates that miRNAs participate in the processes of synaptic plasticity and memory (Earls et al., 2012; Gao et al., 2010). We have identified a number of miRNAs, including miR-329, miR-193b, miR-20a miR-296, and miR-130b, were deregulated in H_2O_2-induced primary hippocampal neurons and different strains of AD model mice (Zhang et al., 2014). In addition, based on our results of microarray, miR-206 and miR-132 have been further identified as novel circulating biomarkers for early diagnosis of aMCI patients (Xie et al., 2015). Several lines of evidence have recently been presented to demonstrate that deregulation of miR-195 expression was related with the neurodegenerative diseases (Ding et al., 2016; Mortuza et al., 2014; Zhu et al., 2012). Ding et al. found the serum miR-195 was up-regulated in samples from sporadic PD patients and it might be a non-invasive biomarker for PD diagnosis (Ding et al., 2016). In AD, miR-195 could downregulate amyloid-β production by targeting BACE1 (Zhu et al., 2012). SIRT1, which is indispensable for normal learning, memory, and synaptic plasticity (Xie et al., 2015), has been confirmed to be regulated by miR-195 in human retinal and dermal microvascular ECs following exposure to 25 mmol/l glucose (Mortuza et al., 2014). In this study, among the possible regulators of mfn2 predicted by bioinformatic analysis, the up-regulated miRNAs which had been identified by microarray were further validated by quantitative RT-PCR analysis. As a result, it had been confirmed that the expression of miR-195 was up-regulated in the hippocampus of SAMP8. Finally, we have also revealed that miR-195 directly interacted with the mfn2 3′-UTR and down-regulated mfn2 protein abundance at the post-translational level *in vitro*. These results indicated that miR-195 was an upstream regulator of mfn2 expression in the progression of AD at least in part.

Both miR-195 and miR-15b belong to miR-16/15/195/424/497 family, which has been shown to play important roles in tumorigenesis and diabetes. Their trends of expression were consistent or opposite under different conditions. For example, puerarin attenuated cardiac hypertrophy and increased miR-15b and miR-195 expression in the

mouse cardiac hypertrophy model and in primary cardiomyocytes (Zhang et al., 2016). However, miR-195 was up-regulated, whereas miR-15b was down-regulated in serum from 106 sporadic PD patients (Ding et al., 2016). In this study, the results of microarray showed that miR-195 and miR-15b were up-regulated in the hippocampus of SAMP8 mice. But the quantitative real-time PCR results showed that the miR-195 levels were increased and miR-15b levels were decreased in hippocampus SAMP8 mice. We speculated that the following reasons lead to inconsistent results in microarray and quantitative real-time PCR: (1) The accuracy of real time quantitative PCR is better than that of the microarray. (2) There might be some individual differences in animal models.

As mentioned above, mitochondrial dysfunction has been involved in the pathogenesis of AD. Accumulating data in the literature have suggested that mfn2 deficiency reduced MMP, an indicator of mitochondrial function (Martorell-Riera et al., 2014; Sebastian et al., 2012). Some studies have indicated mitochondrial ATP content and mitochondrial GSH content decreased gradually in the hippocampi of SAMP8 mice (Shi et al., 2010). Other study showed an increased mitochondrial DNA deletion in the brain of SAMP8 (Fujibayashi et al., 1998). In addition, dissociated brain cells isolated from SAMP8 mice showed significantly reduced MMP and ATP levels (Eckert et al., 2013). We have found the expression of mfn2 was decreased in the hippocampus of SAMP8 mice, and miR-195 was a regulator for mfn2. Thus, whether the deregulation of miR-195 could affect mitochondrial dysfunction by down-regulation of mfn2? The results of fluorescent probe JC-10 staining confirmed that miR-195 induced the loss of MMP in HT-22 cells. Moreover, the reduction of MMP depended on the down-regulated expression of mfn2 protein. These results indicated that deregulation of miR-195 participated in mitochondrial dysfunction by targeting mfn2.

It should be mentioned that mfn2 expression might be regulated by other miRNAs in hippocampus as one mRNA could be targeted by multiple miRNAs. So, further investigations are needed to explore whether other miRNAs could co-regulate the expression and function of mfn2 in AD development. In addition, another limitation of the present study was the absence of experiments to investigate the effect of miR-195 on the cognitive functions by targeting mfn2 *in vivo*. Anyway, our results indicated that mfn2 is a key protein modulated by miR-195 in the development of AD.

In summary, the present study demonstrated that deregulation of mfn2 played a critical role in the mitochondrial disorder during the progression of AD, and its decreased expression was regulated at least in part by miR-195. Therefore, upregulation of mfn2 expression by decreasing the level of miR-195 might be a potential new therapeutic strategy for treatment of AD.

4. Materials and methods

4.1. Animals

SAMP8 and SAMR1 mice aged 3-, 6- and 9- months were obtained from the Animal Center of Beijing University Medical Department. Animals were kept under constant environmental conditions (temperature, 22 ± 2 °C; humidity, 55 ± 5%; 12-/12-h light/dark cycle) with free access to food and water. All experimental procedures were approved by the Animal Care and Use Committee of the First Hospital of Hebei Medical University.

4.2. Cell culture

HT-22 hippocampal neuronal cells and human embryonic kidney 293A cells were purchased from Life Technologies (Waltham, MA, USA) and American Type Culture Collection (ATCC, Manassas, VA, USA), respectively. Cells were cultured in complete Dulbecco's Modification of Eagle's Medium (DMEM) supplemented with 10% fetal bovine serum.

4.3. Quantitative real-time RT-PCR

Total RNAs were isolated from hippocampus of SAMR1 and SAMP8 mice or culture cells with TRIZOL regent (Invitrogen, Burlington, ON, Canada). Reverse transcription reactions were performed using the FastQuant RT Kit (with gDNase) (Tiangen, Beijing, China). Real-time qPCR assay was performed with SuperReal PreMix Plus (SYBR Green) (Tiangen, Beijing, China) using the ABI 7500 sequence detection system (Applied Biosystems, USA), and the data were normalized to the housekeeping gene GAPDH.

MiRNAs were extracted from the hippocampus of SAMR1 and SAMP8 or culture cells with miRcute miRNA Isolation Kit (Tiangen, Beijing, China). Reverse transcription reactions were performed using the miRcute miRNA First-Strand cDNA Synthesis Kit and miRNA specific RT primer (Tiangen, Beijing, China). Real-time qPCR assay was performed with miRcute miRNA qPCR Detection kit (SYBR Green) (Tiangen, Beijing, China) using the ABI 7500 sequence detection system (Applied Biosystems, USA), and the data were normalized to U6 snRNA.

4.4. Protein extraction and western blot analysis

Total protein from tissue samples or HT-22 cells transfected with miR-195 mimics/inhibitor were extracted with protein lysis buffer (150 mM NaCl, 1% NP-40 and 50 mM Tris-HCl, pH 8.0) supplemented with a protease inhibitor cocktail (2 μg/mL phenylmethanesulfonyl fluoride, 2 μg/mL pepstain, 2 μg/mL aprotinin, and 2 μg/mL leupeptin). After being lysed on ice for 30 min, lysates were centrifuged at 12,000 rpm for 20 min, and the supernatant was collected. The protein concentration was measured with a BCA kit. Lysates (50 μg) were resolved by 10% sodium dodecyl sulfate polyacrylamide gel electrophoresis (SDS-PAGE), and the gel was transferred onto a nitrocellulose membrane. The protein on the membranes was detected with rabbit anti-mfn2 (Cat.ab56889, abcam; diluted 1:1000 in PBS) or a mouse monoclonal β-actin antibody (Cat. A5441, Sigma; diluted 1:1000 in PBS) as a loading control. The membranes were then incubated for 1 h at room temperature with a 1: 5000 dilution of anti-mouse/horseradish peroxidase (Santa Cruz Biotechnology, USA) and developed with the Chemiluminescence Plus Western Blot Analysis kit (Santa Cruz Biotechnology, USA).

4.5. Immunohistochemistry

The hippocampal tissue sections were immunohistochemically stained for mfn2 using rabbit primary anti-mfn2 antibody (1:100; Cat.ab56889, abcam USA) and secondary goat anti-rabbit IgG (DBA, Milan, Italy). These methods have been previously described (Kelso et al., 2011). The optical density was measured using Image-Pro Plus 6.0.

4.6. Transfection with miRNA mimic or inhibitor

HT-22 cells were transfected with miR-195 mimic (100 nmol/L) or inhibitor (100 nmol/L) (Guangzhou, China) using Lipofectamine^{2000} (Invitrogen). Scrambled controls were used in parallel. The mfn2 adenovirus was a gift from Dr Song GY (Department of Internal Medicine, Hebei General Hospital).

4.7. Construction of 3′-UTR reporter plasmid and dual luciferase assay

The luciferase vectors including 3′-UTR of mfn2 mRNA (1, 983 bp) (WT-mfn2 or MT-mfn2 vector) were purchased from NorClone Biotech (shanghai, China). Scrambled controls, miR-195 mimic, miR-195

inhibitor, and miR-195 antagomir were obtained from Ribo Bio (Guangzhou, China). Plasmid DNA (WT-mfn2 or MT-mfn2 vector) and miR-195 mimic, miR-195 inhibitor, or scrambled controls were co-transfected into 293A for 24 h. Luciferase activity was measured using the Dual Luciferase Reporter Assay System (Promega, Madison, WI, USA). The experiments were performed in triplicate.

4.8. In vivo *miRNA transfer*

Six-month-old SAMP8 mice (n =12; 6 in each group) underwent infusion with 3 nmol miR-195 antigomir or a scramble control in the lateral ventricle by use of a dental drill. The stereo position of the brain was used to access the exact location of the lateral ventricle. SAMP8 mice anesthetized with 10% chloral hydrate (4 mL/kg) were fixed in a stereotaxic apparatus. The scalp was deflected and a hole drilled through the skull over the injection site. The injection coordinates for the ICV injection were 0.5 mm posterior to the bregma and 1.0 mm to the right or left of the sagittal suture. A 30 gauge needle was dropped to 2.0 mm and a 2 μl mix of miR-195 antagomir and Lipofectamine^{2000} was given over 60 s. The needle was removed, the scalp was closed and the mice were returned to their cages. Mice were sacrificed 48 h after the infusion for detection of gene expression (Cheng et al., 2007).

4.9. *Measurement of mitochondrial membrane potential (MMP)*

After transfected with miR-195 mimic, scrambled controls, or the combination of miR-195 mimic and AD-mfn2 for 24 h, the mitochondrial membrane potential was assessed by Mitochondria Membrane Potential Kit (Cat. MAK159, Sigma, USA) according to the manufacturer's instructions.

4.10. *Statistical analysis*

Statistical analyses were performed by SPSS software version 16.0 (SPSS, Inc., Chicago, IL, USA). Data are expressed as the means ± SD of at least three independent experiments. Comparisons were made using ANOVA for three parametric groups. Student's *t* test was used for two parametric groups. Differences were considered statistically significant at $P < 0.05$.

Conflict of interest

The authors declare no conflict of interest.

Author contributions

RZ: Designed, supervised studies, interpreted results, and prepared the manuscript.

HMZ: Participated in the design of the research and data analysis.

YRM and XMC: Carried out molecular techniques and participated in the analysis of results.

LJ and HW: Participated animal models and the analysis of results.

BX and QFZ: Participated in the research and interpreted results.

DSC: Participated in the research.

SJX: Participated in the design of the research and revised the manuscript.

Acknowledgments

This work was supported by the Hebei Provincial Natural Science Foundation (H2014206406 and H2014206326), China.

References

Bach, D., Pich, S., Soriano, F.X., Vega, N., Baumgartner, B., Oriola, J., Daugaard, J.R., Lloberas, J., Camps, M., Zierath, J.R., Rabasa-Lhoret, R., Wallberg-Henriksson, H., Laville, M., Palacin, M., Vidal, H., Rivera, F., Brand, M., Zorzano, A., 2003. Mitofusin-2 determines mitochondrial network architecture and mitochondrial metabolism. A novel regulatory mechanism altered in obesity. J. Biol. Chem. 278, 17190–17197, (PMID: 12598526).

Bartel, D.P., 2009. MicroRNAs: target recognition and regulatory functions. Cell 136, 215–233, (PMID: 19167326).

Bucha, S., Mukhopadhyay, D., Bhattacharyya, N.P., 2015. Regulation of mitochondrial morphology and cell cycle by microRNA-214 targeting Mitofusin2. Biochem. Biophys. Res. Commun. 465, 797–802, (PMID: 26307536).

Chen, H., McCaffery, J.M., Chan, D.C., 2007. Mitochondrial fusion protects against neurodegeneration in the cerebellum. Cell 130, 548–562, (PMID: 17693261).

Chen, K.H., Guo, X., Ma, D., Guo, Y., Li, Q., Yang, D., Li, P., Qiu, X., Wen, S., Xiao, R.P., Tang, J., 2004. Dysregulation of HSG triggers vascular proliferative disorders. Nat. Cell Biol. 6, 872–883, (PMID: 15322553).

Chen, Y., Han, S., Huang, X., Ni, J., He, X., 2016. The protective effect of icariin on mitochondrial transport and distribution in primary hippocampal neurons from 3x Tg-AD mice. Int J. Mol. Sci., 17, (PMID: 26828481).

Cheng, H.Y., Papp, J.W., Varlamova, O., Dziema, H., Russell, B., Curfman, J.P., Nakazawa, T., Shimizu, K., Okamura, H., Impey, S., Obrietan, K., 2007. microRNA modulation of circadian-clock period and entrainment. Neuron 54, 813–829, (PMID: 17553428).

Colangelo, V., Schurr, J., Ball, M.J., Pelaez, R.P., Bazan, N.G., Lukiw, W.J., 2002. Gene expression profiling of 12633 genes in Alzheimer hippocampal CA1: transcription and neurotrophic factor down-regulation and up-regulation of apoptotic and pro-inflammatory signaling. J. Neurosci. Res. 70, 462–473, (PMID: 12391607).

Corrado, M., Scorrano, L., Campello, S., 2012. Mitochondrial dynamics in cancer and neurodegenerative and neuroinflammatory diseases. Int. J. Cell Biol. 2012, 729290, (PMID: 22792111).

Ding, H., Huang, Z., Chen, M., Wang, C., Chen, X., Chen, J., Zhang, J., 2016. Identification of a panel of five serum miRNAs as a biomarker for Parkinson's disease. Park. Relat. Disord. 22, 68–73, (PMID: 26631952).

Earls, L.R., Fricke, R.G., Yu, J., Berry, R.B., Baldwin, L.T., Zakharenko, S.S., 2012. Age-dependent microRNA control of synaptic plasticity in 22q11 deletion syndrome and schizophrenia. J. Neurosci. 32, 14132–14144, (PMID: 23055483).

Eckert, G.P., Schiborr, C., Hagl, S., Abdel-Kader, R., Müller, W.E., Rimbach, G., Frank, J., 2013. Curcumin prevents mitochondrial dysfunction in the brain of the senescence-accelerated mouse-prone 8. Neurochem. Int. 62, 595–602, (PMID: 23422877).

Fujibayashi, Y., Yamamoto, S., Waki, A., Konishi, J., Yonekura, Y., 1998. Increased mitochondrial DNA deletion in the brain of SAMP8, a mouse model for spontaneous oxidative stress brain. Neurosci. Lett. 254, 109–112, (PMID: 9779932).

Gan, X., Huang, S., Wu, L., Wang, Y., Hu, G., Li, G., Zhang, H., Yu, H., Swerdlow, R.H., Chen, J.X., Yan, S.S., 2014. Inhibition of ERK-DLP1 signaling and mitochondrial division alleviates mitochondrial dysfunction in Alzheimer's disease cybrid cell. Biochim. Biophys. Acta 1842, 220–231, (PMID: 24252614).

Gao, J., Wang, W.Y., Mao, Y.W., Gräff, J., Guan, J.S., Pan, L., Mak, G., Kim, D., Su, S.C., Tsai, L.H., 2010. A novel pathway regulates memory and plasticity via SIRT1 and miR-134. Nature 466, 1105–1109, (PMID: 20622856).

Gao, Q., Wang, X.M., Ye, H.W., Yu, Y., Kang, P.F., Wang, H.J., Guan, S.D., Li, Z.H., 2012. Changes in the expression of cardiac mitofusin-2 in different stages of diabetes in rats. Mol. Med. Rep. 6, 811–814, (PMID: 22825027).

Guo, H., Ingolia, N.T., Weissman, J.S., Bartel, D.P., 2010. Mammalian microRNAs predominantly act to decrease target mRNA levels. Nature 466, 835–840, (PMID: 20703300).

Guo, X., Chen, K.H., Guo, Y., Liao, H., Tang, J., Xiao, R.P., 2007. Mitofusin 2 triggers vascular smooth muscle cell apoptosis via mitochondrial death pathway. Circ. Res. 101, 1113–1122, (PMID: 15322553).

Hailey, D.W., Rambold, A.S., Satpute-Krishnan, P., Mitra, K., Sougrat, R., Kim, P.K., Lippincott-Schwartz, J., 2010. Mitochondria supply membranes for autophagosome biogenesis during starvation. Cell 141, 656–667, (PMID: 20478256).

Hollenbeck, P.J., Saxton, W.M., 2005. The axonal transport of mitochondria. J. Cell Sci. 118, 5411–5419, (PMID: 16306220).

Kelso, M.L., Liput, D.J., Eaves, D.W., Nixon, K., 2011. Upregulated vimentin suggests new areas of neurodegeneration in a model of an alcohol use disorder. Neuroscience 197, 381–393, (PMID: 21958862).

Knott, A.B., Bossy-Wetzel, E., 2008. Impairing the mitochondrial fission and fusion balance: a new mechanism of neurodegeneration. Ann. N.Y. Acad. Sci. 1147, 283–292, (PMID: 19076450).

Liu, W., Liu, C., Zhu, J., Shu, P., Yin, B., Gong, Y., Qiang, B., Yuan, J., Peng, X., 2012. MicroRNA-16 targets amyloid precursor protein to potentially modulate Alzheimer's-associated pathogenesis in SAMP8 mice. Neurobiol. Aging 33, 522–534, (PMID: 20619502).

Manczak, M., Calkins, M.J., Reddy, P.H., 2011. Impaired mitochondrial dynamics and abnormal interaction of amyloid beta with mitochondrial protein Drp1 in neurons from patients with Alzheimer's disease: implications for neuronal damage. Hum. Mol. Genet. 20, 2495–2509, (PMID: 21459773).

Martorell-Riera, A., Segarra-Mondejar, M., Muñoz, J.P., Ginet, V., Olloquequi, J., Pérez-Clausell, J., Palacín, M., Reina, M., Puyal, J., Zorzano, A., Soriano, F.X., 2014. Mfn2 downregulation in excitotoxicity causes mitochondrial dysfunction and delayed neuronal death. EMBO J. 33, 2388–2407, (PMID: 25147362).

Misko, A.L., Sasaki, Y., Tuck, E., Milbrandt, J., Baloh, R.H., 2012. Mitofusin2 mutations disrupt axonal mitochondrial positioning and promote axon degeneration. J. Neurosci. 32, 4145–4155, (PMID: 22442078).

Montecchiani, C., Pedace, L., Lo Giudice, T., Casella, A., Mearini, M., Gaudiello, F., Pedroso, J.L., Terracciano, C., Caltagirone, C., Massa, R., St, George-Hyslop, P.H., Barsottini, O.G., Kawarai, T., Orlacchio, A., 2016. ALS5/SPG11/KIAA1840 mutations cause autosomal recessive axonal Charcot-Marie-Tooth disease. Brain

139, 73–85, (PMID: 26556829).
Mortuza, R., Feng, B., Chakrabarti, S., 2014. miR-195 regulates SIRT1-mediated changes in diabetic retinopathy. Diabetologia 57, 1037–1046, (PMID: 24570140).
Park, J., Choi, H., Min, J.S., Kim, B., Lee, S.R., Yun, J.W., Choi, M.S., Chang, K.T., Lee, D.S., 2015. Loss of mitofusin 2 links beta-amyloid-mediated mitochondrial fragmentation and Cdk5-induced oxidative stress in neuron cells. J. Neurochem. 132, 687–702, (PMID: 25359615).
Sebastián, D., Hernández -Alvarez, M.I., Segalés, J., Sorianello, E., Muñoz, J.P., Sala, D., Waget, A., Liesa, M., Paz, J.C., Gopalacharyulu, P., Orešič, M., Pich, S., Burcelin, R., Palacin, M., Zorzano, A., 2012. Mitofusin 2 (Mfn2) links mitochondrial and endoplasmic reticulum function with insulin signaling and is essential for normal glucose homeostasis. Proc. Natl. Acad. Sci. USA 109, 5523–5528, (PMID: 22427360).
Shi, C., Xiao, S., Liu, J., Guo, K., Wu, F., Yew, D.T., Xu, J., 2010. Ginkgo biloba extract EGb761 protects against aging-associated mitochondrial dysfunction in platelets and hippocampi of SAMP8 mice. Platelets 21, 373–379, (PMID: 20459350).
Soriano, F.X., Liesa, M., Bach, D., Chan, D.C., Palacín, M., Zorzano, A., 2006. Evidence for a mitochondrial regulatory pathway defined by peroxisome proliferator-activated receptor-gamma coactivator-1 alpha, estrogen-related receptor-alpha, and mitofusin 2. Diabetes 55, 1783–1791, (PMID: 16731843).
Takeda, T., Hosokawa, M., Higuchi, K., 1997. Senescence-accelerated mouse (SAM): a novel murine model of senescence. Exp. Gerontol. 32, 105–109, (PMID: 9088907).
Wang, W., Xie, Q., Zhou, X., Yao, J., Zhu, X., Huang, P., Zhang, L., Wei, J., Xie, H., Zhou, L., Zheng, S., 2015. Mitofusin-2 triggers mitochondria Ca2+ influx from the endoplasmic reticulum to induce apoptosis in hepatocellular carcinoma cells. Cancer Lett. 358, 47–58, (PMID: 25541060).
Wang, X., Su, B., Lee, H.G., Li, X., Perry, G., Smith, M.A., Zhu, X., 2009. Impaired balance of mitochondrial fission and fusion in Alzheimer's disease. J. Neurosci. 29, 9090–9103, (PMID: 19605646).
Xie, B., Zhou, H., Zhang, R., Song, M., Yu, L., Wang, L., Liu, Z., Zhang, Q., Cui, D., Wang, X., Xu, S., 2015. Serum miR-206 and miR-132 as potential circulating biomarkers for mild cognitive impairment. J. Alzheimers Dis. 45, 721–731, (PMID: 25589731).
Zhang, R., Han, M., Zheng, B., Li, Y.J., Shu, Y.N., Wen, J.K., 2010. Kruppel-like factor 4 interacts with p300 to activate mitofusin 2 gene expression induced by all-trans retinoic acid in VSMCs. Acta Pharmacol. Sin. 31, 1293–1302, (PMID: 20711222).
Zhang, R., Zhang, Q., Niu, J., Lu, K., Xie, B., Cui, D., Xu, S., 2014. Screening of microRNAs associated with Alzheimer's disease using oxidative stress cell model and different strains of senescence accelerated mice. J. Neurol. Sci. 338, 57–64, (PMID: 24423585).
Zhang, X., Liu, Y., Han, Q., 2016. Puerarin attenuates cardiac hypertrophy partly through increasing Mir-15b/195 expression and suppressing non-canonical transforming growth factor beta (Tgfbeta) signal pathway. Med. Sci. Monit. 22, 1516–1623, (PMID: 27145790).
Zhang, Y., Yang, L., Gao, Y.F., Fan, Z.M., Cai, X.Y., Liu, M.Y., Guo, X.R., Gao, C.L., Xia, Z.K., 2013. MicroRNA-106b induces mitochondrial dysfunction and insulin resistance in C2C12 myotubes by targeting mitofusin-2. Mol. Cell Endocrinol. 381, 230–240, (PMID: 23954742).
Zhao, T., Huang, X., Han, L., Wang, X., Cheng, H., Zhao, Y., Chen, Q., Chen, J., Xiao, R., Zheng, M., 2012. Central role of mitofusin 2 in autophagosome-lysosome fusion in cardiomyocytes. J. Biol. Chem. 287, 23615–23625, (PMID: 22619176).
Zhu, H.C., Wang, L.M., Wang, M., Song, B., Tan, S., Teng, J.F., Duan, D.X., 2012. MicroRNA-195 downregulates Alzheimer's disease amyloid-beta production by targeting BACE1. Brain Res. Bull. 88, 596–601, (PMID: 22721728).